Molecular dynamics simulation and Machine Learning Models for Predicting Welding and Tensile Properties of Diffusion-welded Aluminum-Nickel

M Zaenudin[1], Dian Nugraha[2], Safira Faizah[3], Adhes Gamayel[4], and MN Mohammed[5]*

[1,4]Department of Mechanical Engineering, Faculty of Engineering and Computer Science, Jakarta Global University, Boulevard Raya St. No 2, Tirtajaya, Sukmajaya, Depok 16412, Indonesia

[2,3]Department of Informatics Engineering, Faculty of Engineering and Computer Science, Jakarta Global University, Boulevard Raya St. No 2, Tirtajaya, Sukmajaya, Depok 16412, Indonesia

[5]Department Mechanical Engineering, College of Engineering, Gulf University Sanad 26489, Bahrain

Emails: mzaenudin@jgu.ac.id[1], dian@jgu.ac.id[2], safirafaizah@jgu.ac.id[3], adhes@jgu.ac.id, dr.mohammed.alshekhly@gulfuniversity.edu.bh[5]

ABSTRACT

In this study, machine learning (ML) models are developed to predict the value of interfacial region thickness (IRT) and ultimate tensile strength (UTS) of diffusion-bonded Al-Ni based on molecular dynamics simulation data. Molecular dynamics simulations are performed to simulate the diffusion bonding of Al-Ni with three parameters with three to four level for each parameter. The results of the simulations that are used to generate the ML models are the value of IRT and UTS. The temperature have influenced the performance of ML models with significant impact, indicated by the value of MSE and R^2 that used temperature as the input parameters with an excellent performance. However, the combination of the three parameters as the input shows the best performance, indicated by the MSE value of 0 and the R^2 value of 1, showing that the ML models

performance will increase with the increase of the input data. Furthermore, the models with the highest performance throughout the test are the NN models, followed by the kNN, whereas the other three models showing average performance. This study has successfully developed ML models to predict the IRT and UTS from the molecular dynamics simulation data of diffusion bonding of Al-Ni.
Keywords: molecular dynamics simulation; machine learning models; diffusion welding; aluminum-nickel; tensile behavior

1.0 INTRODUCTION

In many manufacturing processes, there are always activities that involved additive manufacturing to form a material additively, machining to form material by decreasing it, and welding to bond two or more materials [1]. The three activities have their own characteristics, thus have a different advantages and disadvantages. The distinction between additive manufacturing and machining is now spread across the studies, where additive manufacturing that mostly involve 3D printing technology focused on an application that is not require high strength, and the machining process is applied for those that require high strength [2–4]. Meanwhile, the study of welding is related to the activities where the joining of two similar or dissimilar materials is involved [5]. The process focused on producing high quality join, indicated by the low residue of welding which then also increase the physical properties and how strong the bonding between the two welded materials [6–9]. The later manufacturing processes, that is welding, have several difficulties related to the materials properties being joined, since some materials is easily welded, whilst the other is hard, if not impossible. This problem opens wide range of the development of welding techniques [10–13]. One of the welding techniques that can join almost every type of materials is diffusion welding, sometimes also known as diffusion bonding [14–20]. The techniques involved heat and pressure, where the heating phase is not necessarily very high, since the diffusion welding categorized as solid-state welding, and the pressure applied is sometimes very high. In a simplified manner, the diffusion welding process is as follows: the as-received materials are undergoing a heating phase, where it reaches up to about $0.5T_m$ (T_m melting temperature of the materials), then a pressure is applied to one or two side of materials to introduce bonding between the two materials' surfaces [10,21]. This way, there are no filler needed

for the welding, in which it is necessary in the classical welding method that involve fusion and arc. Furthermore, the application of this welding method is vast, not only for joining metallic materials such as steels and metallic alloys, but also for joining glassy, polymer, ceramic, and so forth.

In the presence of computational study, as a frontier and complementary research in the field of materials science, the number of research that utilize computational method is increasing [14,22]. These studies involved significantly different approach and scale, from sub-atomic scale, to the macro scale, from single crystal to polycrystal. The joining between two materials is also an important aspect in terms of computational study that utilize several different computational methods to study behavior and mechanism during the joining process and its properties, thus allowing a faster obtaining results and predict the results from other events outside the experimental data available. Nowadays, there are several computational methods that commonly used, such as quantum and classical molecular dynamics (MD) [23], Monte Carlo (MC) [24], finite element method (FEM) [25,26], phase-field (PF) [27–29], and crystal plasticity (CP) [30,31]. These methods have different purpose, and sometimes scale. For example, the quantum molecular dynamics focused on the first principle study, allowing researcher to determine the properties of a material in a sub-atomic manner which can be used for a bigger scale study such as classical molecular dynamics [32–34]. Classical molecular dynamics focused on the behavior and properties of chunks of atoms where the scale of the study is in nanometer-sized, and the timescale is around pico- to nanosecond [14,22]. Meanwhile, Monte Carlo simulation can complement and/or substitute the use of molecular dynamics simulation, although the method used sometimes different from one to the other researcher. The FEM, PF, and CP studies, the scale is brought to the continuum size where the timescale is in millisecond to second. In case of classical molecular dynamics, the number of studies that utilize this method in the study of joining process is quite high and increasing. From one standpoint, where a basic structural change and the mechanism underlying the process, to the estimation of properties obtained from the quantitation of structural atomic displacement, molecular dynamics have shown its ability to unravel in a deeper manner that is too complex to be observed experimentally. Therefore, the molecular dynamics study is one of the common methods to study a materials behavior at atomic scale with

relatively low in cost and time needed, including studying the behavior of materials during joining processes.

On the other hand, in the age of Artificial Intelligence (AI) [35], and subsequently the development Machine Learning (ML) algorithm [36-38], the research in the field of materials science have developed in such an increasing pace by incorporating various ML techniques, allowing the limitless application of the method. For example, in materials discovery, several studies have shown promising results by incorporating ML, from materials design to the knowledge discovery based on the materials database across the internet [39–42]. Moreover, the prediction of properties of materials by using ML is advantageous, because one does not need to study the entire parameter, but rather study a small number of parameters, then let the various machine learning methods predict the results [43–47]. Even though in some cases it can come in handy, the use of ML for materials research has several drawbacks, such as (a) the dependence in data which also means the data must be clean and have the least error possible, (b) overfitting when the developed model is too complex to search for the underlying pattern, and (c) sometimes high computational resource is necessary. Therefore, the ML method must be adopted carefully and a study to confirm the results is necessary.

In this research, the focus revolves on the leveraging a diverse array of machine learning (ML) models to predict the material properties of diffusion-welded Aluminum and Nickel. The main methodology in supporting the study is the utilization of Molecular Dynamics (MD) simulation results as the primary dataset for constructing the ML model. A comparative analysis is conducted, evaluating the consistency of several prevalent ML models in the predictive task. Among the models developed are k-Nearest Neighbor (kNN), Support Vector Machine (SVM), Linear Regression (LR), Neural Network (NN), and Random Forest (RF). Each model undergoes thorough assessment to study its performance and suitability for the specific predictive task, they are predicting welded material properties. A comprehensive performance of the dataset utilized and its processing procedures is carefully depicted in a supplementary file, ensuring transparency and reproducibility in the research methodology. Through this comparative analysis, the study aim to elucidate the strengths and weaknesses of various ML techniques in predicting the material properties of diffusion-welded Aluminum and Nickel, thereby advancing the frontier of predictive modeling in materials science.

2.0 METHOD

The research methodology involves a systematic approach encompassing multiple stages as depicted in Figure 1. Initially, we construct single crystalline samples of Aluminum (Al) and Nickel (Ni) to serve as the basis for our simulation model. By utilizing molecular dynamics simulation, we carefully simulate the diffusion bonding process by precisely configuring the simulation parameters to generate dump data reflecting the atomic positions at the interface of the two materials. This step is crucial in understanding the intricate atomic interactions and bonding mechanisms between Al and Ni under varying temperature and pressure conditions. The dump file generated is also used for the later estimation of Interfacial Region Thickness (IRT).

Subsequently, the simulation continue with performing of tensile tests on the diffusion-bonded Al-Ni samples to capture their stress-strain behavior. Subsequently, we analyze the dump data extracted from the simulation to estimate the IRT, which, combined with the stress-strain data, facilitates the derivation of critical metrics such as the Ultimate Tensile Strength (UTS). Furthermore, employing a diverse array of machine learning models, including kNN, SVM, LR, NN, and RF, we rigorously evaluate the performance of these models against the simulation-derived dataset. This particular approach not only enhances our comprehension of the Al-Ni bonding process but also provides valuable insights into optimizing material properties through predictive modeling, thereby fostering advancements in materials science and engineering.

2.1 Molecular Dynamics Model(s) and Parameters

The simulation model is consisting of two FCC metal slabs of Ni and Al. A single layer of the Ni-Al slab is located in each end of the slab as fix atom region. It is reasonable to put fix atoms because of the needs of boundary of the two slabs that acts as a boundary. In all three directions (i.e. *x*, *y*, and *z*) periodic boundary is applied, since the NPT (i.e. isothermal-isobaric) ensemble which known as the ensemble that has the most similarity condition with the experimental work in software package LAMMPS [23] that used in this study can only be used if the boundary condition is set to periodic. There are other ensembles that could be use, they are canonical (NVT) and micro-canonical (NVE), but in that two ensembles the pressure parameter cannot be applied and controlled. The choose of the ensemble condition is based on these two reasons, that are the similarity to

the condition of experimental work and the applicable of pressure parameter. Fig. 2(a) and Fig. 2(b) shown the system consists of Al (red) and Ni (blue) slab with dimension of approximately 7.2 nm × 9.2 nm × 9.2 nm for both Ni and Al slabs and followed by fix slab in each edge of the material (cream white and white). Lattice constant applied to the mono-crystal Al and Ni is 4.05 Å and 3.52 Å, respectively as investigated by the references [48-50], and is used as the interatomic potential of choice in this study.

For the simulation part, first boundary condition of the simulation is set to periodic in all three directions that are *x*, *y*, and *z* of the models. This setting allows an atom to pass through one side of the cell and enter in the cell from the opposite side with the same velocity, which allows the simulation cell to maintain a constant atom number during the process of deformation. Also, each atom in the simulation cell interacts with the closest neighbour of the remaining atoms, so that the boundary effect on the simulation can be avoided. Meanwhile, to perform a simulation, a statistical ensemble is required to be defined to represent the state of the modelling system. This project will use Isobaric-Isothermal (NPT) with constant particle number, pressure, and temperature. Furthermore, since the algorithm used by LAMMPS is Verlet, which implement MD simulation through the calculation and solution of equation of motion, this algorithm will be adopted in this project.

For the sake of completeness, here the ensemble condition terms are briefly defined. The term of NPT (Number, Pressure, and Temperature) refers to a condition in which the number of atoms, pressure, and temperature inside the simulated system is maintained at fixed predetermined value. For NVE, which stands for Number, Volume and Energy, the number of atoms, volume of the system, and the energy inside in the system are maintained at fixed predetermined value. Another atomic ensemble that mostly used is NVT, which stands for Number, Volume, and Temperature. This NVT setting will maintain the system with predetermined fixed value of number of atoms, volume, and temperature inside the system. In this study, the NPT ensemble is used due to the ability to control the temperature and pressure, which are the critical parameters that will be investigated.

At the initialization process, the pressure is maintained at atmospheric pressure using isobaric-isothermal (NPT) ensemble and the temperature is maintained at room temperature that is about 300 K. At the equilibrium state, the temperature is designed to

be vary from 300 K, 500 K, and 700 K. Meanwhile, the pressure is set at 10 MPa, 50 MPa, 100 MPa, and 150 MPa in *x* direction in each simulation. At the end, the structure is cooled down from the highest temperature, for instance from temperature of 700 K to 300 K to perform a tensile test at temperature of 300 K with a strain rate of 2.64e9/s. The timestep is set to 1 ps. In a detailed manner, Table 1 shows the simulation parameters and their levels, whilst Table 2 shows the simulation matrix of the employed parameters. The term *SX* means that the numbering of condition, hence it will be easier to be mentioned later in the text.

2.2 Data Description of Simulation Results

The results of the simulations are listed in Table 3. It shows the summary of simulation results that consisting of interfacial region thickness which estimated based on the concentration distribution data and ultimate tensile strength. In case of this research, temperature, pressure, and holding time level is considered as the independent variables, while interfacial region thickness and ultimate tensile strength as the dependent variables. The machine learning models are employed to predict the value of the two independent variables from the data they are learning from. The estimation of interfacial region thickness refers to the thickness of the welded interface where the atom from their original region exceeds the value of 5% on their counterpart region [51]. In this study, it is obtained from the atomic simulation data, where the geometric location of the atoms is extracted in a dump file, thus allowing the estimation of their thickness of the interfacial region by the utilization of Python code. On the other hand, the estimation of ultimate tensile strength is defined by the maximum value of stress obtained from the Stress-Strain curve generated directly from the simulation by using ‘fix deform’ code included in LAMPPS package, i.e. the tensile test simulation.

The difference in the input parameters, they are temperature, pressure, and holding time, in subjecting Aluminum and Nickel for diffusion welding has shown to have significant impact in their as-welded properties. In our study, two parameters are employed to determine the performance of the as welded materials through estimation and testing, they are interfacial region thickness and tensile strength. In the welding process, the temperature within the system temperature firstly raised into certain value and maintained for a certain time (holding time) while pressure with certain value is

applied from both direction to promote bonding between the two materials. This phenomenon is confirmed from previous study related to diffusion welding of Al-Ni, whether the Al-Ni as the main materials or Ni as the filler for the welding, since Ni is one of the most used filler materials in terms of diffusion welding. Although, in some cases, diffusion welding tends to reduce the use of filler material, however for the materials that are known as hard to be welded, filler material is necessary. For example, by using Ni multilayer for Al/Steel joint, the tensile performance is 3 times higher than that of the Al/steel joint directly [52]. Also, the use of Al-Ni energetic multilayer shows to improve the chemical reaction upon ultrahigh compressive load [53]. These studies suggests that the diffusion welding of Al-Ni is possible, and that in some cases, the combination of this materials during welding has improved both tensile and compressive strength.

The structural evolution of Aluminum and Nickel during diffusion welding is presented in Fig. 3. The color mapping of the figure describe the displacement magnitude, where the read colored atoms shows the atoms with the highest displacement. It is then concluded that, the higher the level of all of the three parameters, the higher displacement produced by the diffusion welding process, by lookit at the structural evolution and the final results where the simulation time reaching 250 ps. The far right of the figure shows the diffusion interface, where the atoms that reaching the value of 1 nm in displacement will be left, while the other atoms is removed. The interface structure will help us in describing how the interface evolved along the simulation. To determine the interfacial region thickness, a concentration distribution is utilized as the base of the calculation. Concentration distribution defines as the concentration type(s) of atoms along an axis. Typically, in the concentration distribution curve, the atom had a cross-section where it is located at 0 point and rise or fall sharply. It could be used to determine the quality of joint, since the welding depth is shown clearly within this curve. Concentration distribution also can be utilized to calculate interfacial region thickness by estimate the point where a certain amount of atoms are reached in a cross-section area. In our study, the interfacial region thickness is defined as a region where the concentrations of Aluminum and Nickel atoms are both over 5% in the cross-sectional area. Samples of concentration distribution curve is depicted in Fig. 4. Lastly, the stress-strain curve corresponded to the sample S46, S47, and S48 is presented in Fig. 5. The tensile test is one of the basic idea of how to determine the strength of the materials, that is by stressing

or loading the sample gradually until a certain value until the materials reaching failure. From the tensile test process, the value of strain and stress at which the test is performed is recorded in a text file, thus allowing it to be processed later. From the results of the tensile test, it is shown that as the level of the parameters rise, the strength of the as-welded Al-Ni is decreased. From all these data, one may concluded that it is commonly happen in an experimental work, thus the machine learning model shall not find any trouble in predicting the value of interfacial region thickness and tensile strength from the simulation data. However, it is then comes to the aim of this paper to evaluate the common machine learning algorithm in predicting value.

2.3 Machine Learning Models and Settings

In this study, five ML models are employed, they are kNN (k-Nearest Neighbor), SVM (Support Vector Machine), LR (Linear Regression), Neural Network (NN), and RF (Random Forest). These techniques are chosen since they are five of the commonly used ML techniques for the simplest to intermediate use, including in the engineering application like predicting materials' properties [54]. A proper setting of the technique is necessary to produce a correct result of the models developed. In this case, the setting also means to making sure the results are reproducible. The setting of the ML techniques employed is listed in Table 4. From the data in Table 3, the data is train and test by dividing the data into two parts, they are train and test data, whereas in some models, the iteration of the training is also involved. This is a common way in training and testing a machine learning model performance. Moreover, by using this method, no other data is necessary, and the development of the model is thus more efficient. However, it can sometimes have several drawbacks, and one of it is that it cannot be directly implemented with another similar data, since it is different, and a model must be developed for every different cases. Python programming is used as the basis of the developed model. Python is programming language that is now known as one of the most used programming language to develop and train machine learning model, since it has support from various machine learning library, such as TensorFlow (https://www.tensorflow.org/) and PyTorch (https://pytorch.org/), and module such as Orange apps (https://orangedatamining.com/) and Orange library (https://orange3.readthedocs.io).

3.0 RESULTS AND DISCUSSIONS

3.1 Classical Assumption Test

In the world of machine learning (ML) model development, the classical assumption test serves as a foundational pillar, underpinning the reliability and integrity of the further analyses. By subjecting the dataset to a rigorous tests, including but not limited to normality, multicollinearity, and heteroscedasticity test, it helps ensure that the fundamental assumptions of statistical analysis are met [55]. For instance, normality tests are helpful in verifying whether the data distribution adheres to the Gaussian distribution, a critical prerequisite for various statistical techniques. By confirming normality, one can rely on accurate parameter estimates, facilitating more precise predictions and inferences. Similarly, detecting multicollinearity—a condition where predictor variables are highly correlated—helps prevent redundancy in the model and ensures that each variable contributes meaningfully to the prediction task. This, in turn, prevent against biased coefficient estimates and enhances the model's interpretability.

Furthermore, the detection of heteroscedasticity, or the unequal variance of errors across observations, is strongly important for ensuring the robustness of statistical inferences. By identifying and addressing heteroscedasticity, the developers can ensure that the model's predictions remain reliable across different subsets of the data, regardless of variations in sample sizes or other factors. Moreover, adherence to these classical assumptions not only strengthen the accuracy and reliability of machine learning models but also instills confidence in the validity of subsequent analyses and insights derived from it. The classical assumption test can be thought as a critical quality control mechanism, enabling one to build machine learning models on a solid statistical foundation, thereby enhancing their effectiveness and applicability in real-world scenarios.

3.1.1 Normality Test

The normality test plays a crucial role in assessing the distribution of both independent and dependent variables [55]. Fig. 6(a) and Fig. 6(b) depicts the p-plots of the normality tests conducted for the interfacial region thickness and ultimate tensile strength data, respectively. Notably, the data points in both plots are distributed along the diagonal axis of the normal distribution graph, indicating a normal distribution pattern.

This finding suggests that the collected data effectively represent the underlying population, thereby meeting the criteria for normality. However, a closer examination reveals that the ultimate tensile strength data exhibit a higher degree of alignment with the diagonal line compared to the interfacial region thickness data. This discrepancy can be attributed to the nature of data collection processes. For instance, while the ultimate tensile strength data are directly obtained from the simulation process, providing a more standardized measurement approach, the interfacial region thickness data rely on estimations derived from concentration distribution data. Consequently, the latter may introduce some level of error due to the lack of a standardized estimation method. Despite this variability, the regression standardized residual analysis confirms the normal distribution of the data.

3.1.2 Multicollinearity test

Multicollinearity, a phenomenon where two or more independent variables exhibit correlation, poses a challenge in statistical modeling [55]. Ideally, independent variables in a well-constructed model should remain uncorrelated to ensure orthogonality. The presence of multicollinearity can undermine the model's accuracy and interpretability. To assess the presence of multicollinearity symptoms among independent variables, we examine tolerance and variance inflation factor (VIF) values. A VIF value below 10 and a tolerance above 0.1 typically indicate the absence of multicollinearity. As depicted in Table 5, the results of the multicollinearity test reveal no evidence of multicollinearity among the independent variables utilized in this study. It suggests that the trained ML models are likely to exhibit robust performance, benefiting from the absence of multicollinearity-induced biases.

3.1.3 Heteroscedasticity test

In the context of statistical analysis, heteroscedasticity signifies fluctuating error variance within the dataset, posing potential implications for the reliability of significance tests and goodness-of-fit assessments. To ascertain the presence of heteroscedasticity, a scatter plot analysis is employed, serving as a visual diagnostic tool to scrutinize the variability of the data. In this study, the scatter plot method is utilized to evaluate whether the data exhibit any heteroscedasticity. Specifically, deviations such as waviness,

widening, or narrowing in the scatter plot may suggest the presence of heteroscedasticity. In the presented analysis, scatter plots depicting the heteroscedasticity test results for both interfacial region thickness and ultimate tensile strength are illustrated in Fig. 7(a) and Fig. 7(b), respectively. Upon examination of these plots, no pattern emerges for either the interfacial region thickness or ultimate tensile strength data. This absence of pattern signifies a consistent variance across the dataset, indicating the absence of heteroscedasticity within the analyzed data. This observation instills confidence in the reliability of subsequent statistical analyses and model interpretations, ensuring the validity of conclusions drawn from the dataset.

The favorable outcomes of the three tests—normality, multicollinearity, and heteroscedasticity—suggest that the dataset exhibits desirable characteristics, including well-distributed data, absence of multicollinearity, and consistent error variance. These findings imply that the data are suitable for modeling purposes, as they meet fundamental assumptions required for reliable statistical analyses. Specifically, the absence of multicollinearity ensures that the predictor variables are independent, enhancing the accuracy and interpretability of the model estimates. Additionally, the consistent error variance observed indicates that the model's predictions are likely to be unbiased and reliable across different levels of the predictor variables.

With these positive indications, the machine learning model generated from the analyzed data is anticipated to yield accurate estimations, unbiased predictions, and consistent performance. These attributes are essential for ensuring the robustness and validity of the model outputs, enabling informed decision-making based on the model's predictions. Moreover, the confidence in the reliability of the model enhances its applicability in real-world scenarios, where accurate predictions are crucial for guiding various decision-making processes. Overall, the favorable outcomes of the assumption tests provide assurance regarding the quality and suitability of the dataset for developing machine learning models with practical utility and reliability.

3.2 Comparison of Machine Learning Techniques to Predict Mechanical Properties of Diffusion Welded Al-Ni

The comparison on ML techniques in this study is divided into three parts, which is differentiated by the number of independent variables considered as the input for the

generated models in predicting the output. This differentiation is to demonstrate that the strength of ML techniques and its generated models in this study must be also supported by a fair amount of data to train the models. From one independent variable to three independent variables, the variation of performance is discussed in detail. In the tables provided later, there are several performance indicators of a machine learning model, they are mean square error (MSE), root mean square error (RMSE), mean absolute error (MAE), mean absolute percentage error (MAPE), and R^2.The MSE value measures the average of the squared differences between the model prediction and the observed values in the data. Similar to MSE, the RMSE measure the difference of the model prediction and the observed data, but rather it provides a measure of the average error in the same unit as the target variable. MAE measures the average of the absolute differences between the model's predictions and the observed values in the data. Like MAE, MAPE measures the average percentage of absolute errors of the model's predictions against the observed values in the data. Lastly, also known as the coefficient of determination, R^2 measures how well the variability in the target data is explained by the model. The value of R^2 ranges from 0 to 1, where 1 indicates that the model excellently explains the variability in the data, while 0 indicates that the model provides no explanation. In this paper, for comparison purpose, graphs are provided to easily shows the comparison of performance between the models, but instead of includes of all five variables, only two variables are included, they are R^2 and MSE. A higher R^2 value indicates better model performance in explaining data variability, thus showing better performance, while lower MSE values indicate better model performance in predicting the data. The two variables considered to be enough in representing the ML performance in a graph.

3.2.1 One independent to single dependent variables

In a scheme where one independent variable is used to construct a ML models, the performance prediction of dependent variables is relatively low. For example, in Table 6, the value of MSE and R^2 of the temperature parameter in predicting interfacial region thickness (IRT) and ultimate tensile strength (UTS) are varied for every models. NN model with input parameter of temperature performs well with MSE value of 0.531 and R^2 value of 0.837 in predicting IRT, and MSE value of 0.033 and R^2 value of 0.793 in predicting UTS. This model shows the best performance compared to other models,

whilst the least perform model showed by LR. With the input parameters of pressure, in terms of MSE and R^2 value, all the models show a poor performance, which is similar to those models with the input parameters of holding time. This performance showed that, with one input parameters, only temperature parameter is reliable in predicting the value of IRT and UTS from the simulation data. Fig. 8 and Fig. 9 shows the performance characteristics of the five models in predicting IRT and UTS with one independent variable as the input parameter. All the value of R^2 and MSE with the input parameters of pressure and holding time shows a low performance, and only temperature as the input parameters that with all the model well performed.

In most cases, a welding will perform well if only a sufficient amount of heat is involved in the process. The heat will allow the atoms from both materials that will be welded to promote bonding. Until a certain limit, a higher temperature shows a better bonding in most cases of welding, and when the sample is subjected to a test, it shows a better performance in terms of mechanical and physical properties. This phenomenon is confirmed in this study, that is, as the value of the temperature is increased, the performance in terms of IRT and UTS is also increased, and it is predicted by the model developed in this study, whereas the influence of the value of pressure and holding time is relatively low compared to temperature.

3.2.2 Two independents to single dependent variables

Two independent variables are employed to generate models that predicts IRT and UTS. Three possible combinations are Temperature-Pressure, Temperature-Holding Time, and Pressure-Holding Time. The performance of these five models for each parameter combination is presented in Table 7, whilst for Fig. 10 and Fig. 11 shows the graph of models' performance that depicts two variable performances, where Fig. 10 depicts the R^2 performance and Fig. 11 depicts MSE performance. The results show that, two of the three combination of parameters that involved temperature has shown an excellent performance, where the value of MSE and R^2 are ranged from 0.467 – 1.028 and 0.684 – 0.856 in predicting IRT, 0.017 – 0.029 and 0.818 – 0.897 in predicting UTS, respectively. On the other hand, the combination in which does not involve temperature as one of the variables shows a low in performance, both in MSE and R^2, ranged from 2.873 – -0.069 and 0.15 – 0.22, respectively, and in other parameters. This value is

relatively low and thus the model cannot be used for predicting both IRT and UTS. The performances of the combined two parameters as the input in this study explain that the temperature parameters still hold the important effect, that without the use of it as the input parameters, the performance of the models is low. Furthermore, even though temperature with single parameter as the input already shows a well performance, the performance is still increase when a new data is inserted, that is the combination with pressure and holding time. By considering more data involved in the input parameters, a better performance of the model is achieved.

3.2.3 Three independents to single dependent variables

Finally, by combining all three parameters involved in the simulation as the input parameters, an excellent model that predicts both IRT and UTS is generated. For example, in terms of MSE, two of the five models, that is kNN and NN, show a value of 0 which describe that the model can excellently predicts the data. In terms of R^2, the models have a value of 1 for both models, which describe that the model have explained the variability in an outstanding manner. Both the value of MSE and R^2 on the other models, they are SVM, LR, and RF, although not as impressive as the kNN and NN models, still shows a good performance, where the MSE and R^2 value is ranged from 0.029 – 0.777 and 0.749–0.986 (Table 8), respectively, which is quite excellent and can be used as the ML models that predicts properties such as IRT and UTS. In Figure 12(a) and Fig. 12(b), the models' performance is high, where only LR model that has a poor value of MSE in predicting the IRT, which means it will not excellently predict the output data, which is also shows in Fig. 12(a) for R^2 value.

4.0 CONCLUSIONS

The study utilized molecular dynamics simulations to replicate the diffusion welding process of Al-Ni, incorporating three input parameters: temperature, pressure, and holding time, alongside two output parameters: interfacial region thickness (IRT) and ultimate tensile strength (UTS). Detailed discussions have already been conducted on the simulation results and the performance of various machine learning models. The conclusions drawn from the analysis are summarized as follows:

1. The classical assumption test conducted on the dataset demonstrated that the data used for model generation are statistically unbiased and consistent. Consequently, the models developed from this data are expected to provide accurate estimations, enhancing their reliability and validity for predictive purposes.
2. Among the input parameters, temperature shows a significant influence on the predicted values of both IRT and UTS. However, when combined with the other input parameters, the inclusion of more data for training resulted in improved model performance. This suggests that utilization of multiple input parameters enhances the model's ability to capture the complexity of the underlying data, leading to more accurate predictions.
3. The evaluation of various machine learning models revealed that Neural Network and k-Nearest Neighbor yielded the best performance in estimating the values of IRT and UTS. Particularly when all input parameters were considered, these models achieved a mean squared error (MSE) of 0 and a coefficient of determination (R^2) of 1, indicating excellent agreement between the predicted and observed values.

ACKNOWLEDGEMENTS

The authors acknowledge the support from Jakarta Global University and Management & Science University throughout this project.

AUTHORS CONTRIBUTION

Conceptualization and performing simulation, M.Z. and M.N.M.; Data analysis, processing, and machine learning modelling, S.F., M.Z.; Manuscript writing and review, M.Z., D.N., S.F., M.N.M.; Supervision, M.N.M.; Project administration, D.N. and S.F. All authors have read and agreed to the published version of the manuscript.

COMPETING INTEREST

The authors declare no conflict of interest.

DATA AVAILABILITY

The raw data can be obtained upon request from the corresponding author.

REFERENCES

[1] Zhu, Z., Dhokia, V.G., Nassehi A., *et al.*, "A review of hybrid manufacturing processes - State of the art and future perspectives," Int. J. Comput. Integr. Manuf., 26(7), pp. 596–615, (2013). DOI: https://doi.org/10.1080/0951192X.2012.749530

[2] Faludi, J., Bayley, C., Bhogal, S., *et al.*, "Comparing environmental impacts of additive manufacturing vs traditional machining via life-cycle assessment," Laboratory for Manufacturing and Sustainability, (2015). DOI: 10.1108/RPJ-07-2013-0067

[3] Williams, S.W., *et al.*, "Wire+arc additive manufacturing vs. traditional machining from solid: a cost comparison," Materials Science and Technology (United Kingdom), 32(10), (2015).

[4] Hodonou, C., Balazinski, M., Brochu, M., *et al.*, "Material-design-process selection methodology for aircraft structural components: application to additive vs subtractive manufacturing processes," International Journal of Advanced Manufacturing Technology, 103, pp. 1509-1517, (2019). DOI: https://doi.org/10.1007/s00170-019-03613-5

[5] Singhal, T.S., *et al.*, "A comprehensive comparative review: welding and additive manufacturing," International Journal on Interactive Design and Manufacturing, 18(3), pp. 1-15, (2023). DOI: http://dx.doi.org/10.1007/s12008-022-01152-0

[6] Wang, C., Zhang, S., Luo, Z., *et al.*, "High-quality welding of glass by a femtosecond laser assisted with silver nanofilm," Appl. Opt., 60(18), (2021). DOI: https://doi.org/10.1364/ao.422078

[7] Zhang, M., *et al.*, "High-quality dissimilar friction stir welding of Al to steel with no contacting between tool and steel plate," Mater. Charact., 191, (2022). DOI: https://doi.org/10.1016/j.matchar.2022.112128

[8] Kawahito, Y., Mizutani, M., and Katayama, S., "High quality welding of stainless steel with 10 kW high power fibre laser," Science and Technology of Welding and Joining, 14(4), pp. 288-294, (2009). DOI: https://doi.org/10.1179/136217108X372531

[9] Sakagawa, T., Nakashiba, S., Haraguch, S., *et al.*, "High efficiency and high quality welding of aluminum alloy by hybrid system combined Nd: YAG laser and diode

laser," Seimitsu Kogaku Kaishi/Journal of the Japan Society for Precision Engineering, 75(10), pp. 1008-1014, (2009). DOI: https://doi.org/10.2351/1.5061445

[10] Shravan, C., Radhika, N., Deepak Kumar, N. H., *et al.*, "A review on welding techniques: properties, characterisations and engineering applications," Advances in Materials and Processing Technologies, 10(2), pp. 1126-1181, (2023). DIO: https://doi.org/10.1080/2374068X.2023.2186638

[11] Karabulut, G. and Beköz Üllen, N., "A Review on Welding Techniques of Metallic Foams," Erzincan University Journal of Science and Technology, 15(1), pp. 217-232, (2022). DOI: https://doi.org/10.18185/erzifbed.997743

[12] Yu, D., Zhang, Y., Zhou, J., *et al.*, "Joining of titanium-copper TA2/T2 bimetallic sheet by double side laser-TIG welding," International Journal of Materials Research, 113(11), pp. 974-983, (2022). DOI: https://doi.org/10.1515/ijmr-2021-8542

[13] Dakarapu, S. R., Maddili, P. C., and Revu, K. M., "Effect of nanoparticle on mechanical properties of activated tungsten gas welding of austenite stainless steel 316L and optimization of process parameters," International Journal of Materials Research, 114(4–5), pp. 266-275, (2023). DOI: https://doi.org/10.1515/ijmr-2022-0042

[14] Zaenudin, M., Mohammed, M. N., and Al-Zubaidi, S., "Molecular dynamics simulation of welding and joining processes: An overview," International Journal of Engineering and Technology(UAE), 7(4) pp. 3816–3825, (2018). DOI: https://doi.org/10.14419/ijet.v7i4.16610

[15] Zaenudin, M., Mohammed, M. N., and Al-Zubaidi, S., "Atomistic investigation on the effect of temperature on mechanical properties of diffusion-welded Aluminium-Nickel," International Journal of Integrated Engineering, 12(5), pp. 62-69, (2020). DOI: https://doi.org/10.30880/ijie.2020.12.05.008

[16] Zaenudin, M., Mohammed, M. N., Gamayel, A., *et al.*, "Atomistic investigation of diffusion welding of dissimilar materials through molecular dynamics simulation," AIP Conference Proceedings, 2256 (1), 2020. DOI: https://doi.org/10.1063/5.0014466

[17] Zaenudin, M., Mohammed, M.N., and Al-Zubaidi, S., "Atomistic Investigation on Diffusion Bonding between Al and Ni using Molecular Dynamics Simulation," ICSGRC 2019 - 2019 IEEE 10th Control and System Graduate Research Colloquium, Proceeding, pp. 213-218, (2019). DOI: https://doi.org/10.1109/ICSGRC.2019.8837051

[18] Zaenudin, M., Mohammed, M. N., Sunardi, A., *et al.*, "Atomistic investigation on the failure of diffusion-bonded Aluminium-Nickel," Journal of Physics: Conference Series, 1450(1), (2020). DOI: 10.1088/1742-6596/1450/1/012053

[19] Zaenudin, M., Abd Gaffar, A. H., Mohammed, M. N., *et al.*, "Study the Effect of Temperature on the Diffusion Bonding of Cu-Al by Using Molecular Dynamics Simulation," 2019 IEEE International Conference on Automatic Control and Intelligent Systems, I2CACIS 2019 - Proceedings, pp. 345–348, (2019). DOI: https://doi.org/10.1109/I2CACIS.2019.8825068

[20] Zaenudin, M., Abdulrazaq, M. N., Al-Zubaidi, S., *et al.*, "Atomistic Investigation on the Role of Temperature and Pressure in Diffusion Welding of Al-Ni," Journal of Engineering & Technological Sciences, 52(2), pp. 181-196, (2020). DOI: http://dx.doi.org/10.5614/j.eng.technol.sci.2020.52.2.4

[21] Bedjaoui, W., Boumerzoug, Z., and Delaunois, F., "Solid-State Diffusion Welding of Commercial Aluminum Alloy with Pure Copper," International Journal of Automotive and Mechanical Engineering, 19(2), pp. 9734–9746, (2022). DOI: https://doi.org/10.15282/ijame.19.2.2022.09.0751

[22] Zaenudin, M., Mohammed, M. N., and Al-Zubaidi, S., "A Review on Molecular Dynamics Simulation of Joining Carbon-Nanotubes and Nanowires: Joining and Properties," International Journal of Integrated Engineering, 14(4), pp. 137–159, (2022). DOI: https://doi.org/10.30880/ijie.2022.14.04.011

[23] Thompson, A.P., *et al.*, "LAMMPS - a flexible simulation tool for particle-based materials modeling at the atomic, meso, and continuum scales," *Comput Phys Commun*, 271, p. 108171, (2022). DOI: https://doi.org/10.1016/j.cpc.2021.108171

[24] Akkermans, R. L. C., Spenley, N. A., and Robertson, S. H., "Monte carlo methods in materials studio," Mol. Simul., 39(14–15), pp. 1153–1164, (2013). DOI: https://doi.org/10.1080/08927022.2013.843775

[25] Belytschko, T., Gracie, R., and Ventura, G., “A review of extended/generalized finite element methods for material modeling,” Modelling and Simulation in Materials Science and Engineering, 17(4), (2009). DOI: 10.1088/0965-0393/17/4/043001

[26] Bao, G. and Li, P., “Finite Element Methods,” Applied Mathematical Sciences (Switzerland), pp. 87-161, (2022). DOI: 10.1007/978-981-16-0061-6_4

[27] Peng, F., Ma, Y., Huang, W., *et al.*, “Failure analysis of composite materials based on phase field method: A review,” Fuhe Cailiao Xuebao/Acta Materiae Compositae Sinica, 40(5), (2023). DOI: http://dx.doi.org/10.13801/j.cnki.fhclxb.20220818.001

[28] Tonks, M. R. and Aagesen, L. K., “The Phase Field Method: Mesoscale Simulation Aiding Material Discovery,” Annu. Rev. Mater. Res., 49, (2019). DOI: https://doi.org/10.1146/annurev-matsci-070218-010151

[29] Li, Y., Hu, S., Sun, X., *et al.*, “A review: Applications of the phase field method in predicting microstructure and property evolution of irradiated nuclear materials,” npj Computational Materials, 3(16), (2017). DOI: https://doi.org/10.1038/s41524-017-0018-y

[30] Nguyen, K., Zhang, M., Amores, V. J., *et al.*, “Computational modeling of dislocation slip mechanisms in crystal plasticity: A short review,” Crystals (Basel), 11(1), (2021). DOI: https://doi.org/10.3390/cryst11010042

[31] Roters, F. *et al.*, “DAMASK – The Düsseldorf Advanced Material Simulation Kit for modeling multi-physics crystal plasticity, thermal, and damage phenomena from the single crystal up to the component scale,” Comput. Mater. Sci., 158, (2019). DOI: https://doi.org/10.1016/j.commatsci.2018.04.030

[32] Hautier, G., Jain, A., and Ong, S. P., “From the computer to the laboratory: Materials discovery and design using first-principles calculations,” J. Mater. Sci., 47(21), pp. 7317–7340, (2012). DOI: https://doi.org/10.1007/s10853-012-6424-0

[33] Oganov, A. R., Pickard, C. J., Zhu, Q., *et al.*, “Structure prediction drives materials discovery,” Nature Reviews Materials, 4(5), pp. 331–348, (2019). DOI: https://doi.org/10.1038/s41578-019-0101-8

[34] Chesser, I., Koju, R. K., and Mishin, Y., “Atomic-level mechanisms of short-circuit diffusion in materials,” International Journal of Materials Research, 115(2), pp. 85-105, (2024). DOI: https://doi.org/10.1515/ijmr-2023-0202

[35] Cao, L., "A New Age of AI: Features and Futures," IEEE Intell. Syst., 37(1), pp. 25-37, (2022). DOI: https://doi.org/10.1109/MIS.2022.3150944

[36] Azrag, M. A. K., Zain, J. M., Kadir, T. A. A., *et al.*, "Review: machine and deep learning methods in Malaysia for COVID-19," Indonesian Journal of Electrical Engineering and Computer Science, 31(1), pp. 514-520, (2023). DOI: http://doi.org/10.11591/ijeecs.v31.i1.pp514-520

[37] Somashekar, H. and Boraiah, R., "Network intrusion detection and classification using machine learning predictions fusion," Indonesian Journal of Electrical Engineering and Computer Science, 31(2), pp. 1147-1153, (2023). DOI: http://doi.org/10.11591/ijeecs.v31.i2.pp1147-1153

[38] Meenal, R., Michael, P. A., Pamela, D., *et al.*, "Weather prediction using random forest machine learning model," Indonesian Journal of Electrical Engineering and Computer Science, 22(2), pp. 1208-1215, (2021). DOI: http://doi.org/10.11591/ijeecs.v22.i2.pp1208-1215

[39] Tao, Q., Xu, P., Li, M., *et al.*, "Machine learning for perovskite materials design and discovery," npj Computational Materials, 7(1), (2021). DOI: https://doi.org/10.1038/s41524-021-00495-8

[40] Liu, Y., Zhao, T., Ju, W., *et al.*, "Materials discovery and design using machine learning," Journal of Materiomics, 3(3), (2017). DOI: https://doi.org/10.1016/j.jmat.2017.08.002

[41] Oliveira, O.N., and Oliveira, M.C.F., "Materials Discovery With Machine Learning and Knowledge Discovery," Front. Chem., 10, (2022). DOI: https://doi.org/10.3389/fchem.2022.930369

[42] Cai, J., Chu, X., Xu, K., *et al.*, "Machine learning-driven new material discovery," Nanoscale Advances, 2, pp. 3115-3130, (2020). DOI: https://doi.org/10.1039/D0NA00388C

[43] Vivanco-Benavides, L. E., Martínez-González, C. L., Mercado-Zúñiga, C., *et al.*, "Machine learning and materials informatics approaches in the analysis of physical properties of carbon nanotubes: A review," Computational Materials Science, 201. (2022). DOI: https://doi.org/10.1016/j.commatsci.2021.110939

[44] Wang, J., Fa, Y., Tian, Y., *et al.*, "A machine-learning approach to predict creep properties of Cr–Mo steel with time-temperature parameters," Journal of Materials

Research and Technology, 13, 2021. DOI: https://doi.org/10.1016/j.jmrt.2021.04.079

[45] Stoll, A. and Benner, P., "Machine learning for material characterization with an application for predicting mechanical properties," GAMM Mitteilungen, 44(1), (2021). DOI: https://doi.org/10.1002/gamm.202100003

[46] Bhavana, N., and Kodabagi, M. M., "Comprehensive Pothole Detection System for Road Maintenance and Safety Using Image Processing and Stereo Vision," Malaysian Journal of Computer Science, 36(4), pp. 44-53, (2023). DOI: https://doi.org/10.22452/mjcs.sp2023no1.4

[47] Karn, A. L., *et al.*, "Designing A Deep Learning-Based Financial Decision Support System for Fintech to Support Corporate Customer's Credit Extension," Malaysian Journal of Computer Science, 2022(1), pp. 116-131, (2022). DOI: https://doi.org/10.22452/mjcs.sp2022no1.9

[48] Mishin, Y., Mehl, M. J., and Papaconstantopoulos, D. A., "Embedded-atom potential for B2-NiAl," Phys. Rev. B: Condens. Matter. Mater. Phys., 65(22), (2002). DOI: https://doi.org/10.1103/PhysRevB.65.224114

[49] Mishin, Y., "Atomistic modeling of the γ and γ′-phases of the Ni-Al system," Acta. Mater., 52(6), (2004). DOI: https://doi.org/10.1016/j.actamat.2003.11.026

[50] Purja Pun, G. P., and Mishin, Y., "Development of an interatomic potential for the Ni-Al system," Philosophical Magazine, 89(34–36), pp. 3245–3267, (2009). DOI: https://doi.org/10.1080/14786430903258184

[51] Chen, S. D., Soh, A. K., and Ke, F. J., "Molecular dynamics modeling of diffusion bonding," Scr. Mater., 52(11), (2005). DOI: https://doi.org/10.1016/j.scriptamat.2005.02.004

[52] Yu, J., Fan, Y., Zhang, H., *et al.* "Interfacial evolution of thermo-compensated resistance diffusion welding of Al/steel joint with Ni interlayer via resistance seam welding," Journal of Materials Engineering and Performance, 33(13), pp. 6480-6487, (2024). DOI: https://doi.org/10.1007/s11665-023-08418-y

[53] Shen, S., Li, H., Liang, Y., *et al*, "Chemical reactions of Ni/Al multilayers upon ultrahigh compressive load at ambient temperature," Journal of Alloys and Compounds, 968, pp. 172164, (2023). DOI: https://doi.org/10.1016/j.jallcom.2023.172164

[54] Schmidt, J., Marques, M. R., Botti, S., *et al.*, “Recent advances and applications of machine learning in solid-state materials science,” npj. comp mat, 5(1), (2019). DOI: https://doi.org/10.1038/s41524-019-0221-0

[55] Ghozali, I., “Aplikasi analisis multivariate dengan program IBM SPSS 25 edisi ke-9,” Badan Penerbit Universitas Diponegoro, (2018).

List of Figures:

List of Tables:

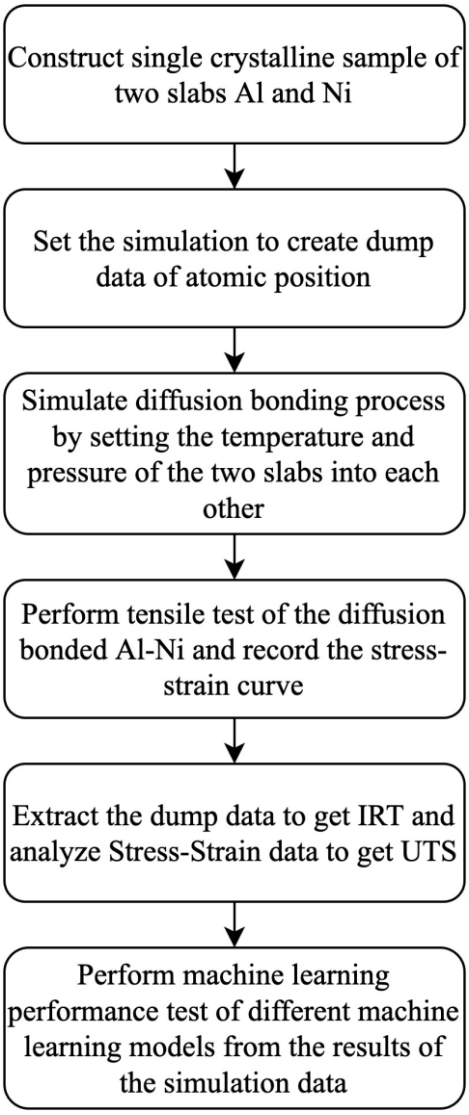

Fig. 1: Flow diagram of the study.

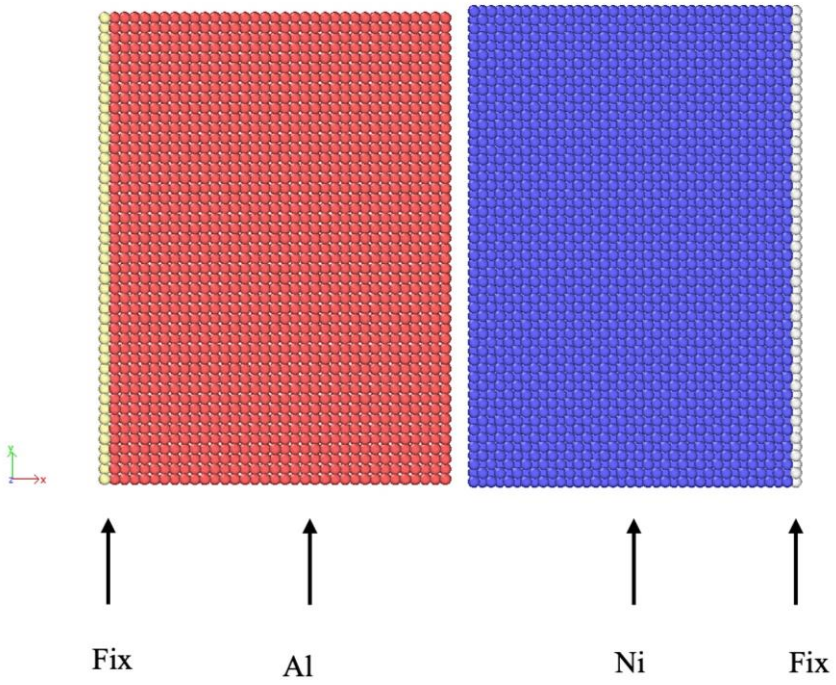

(a)

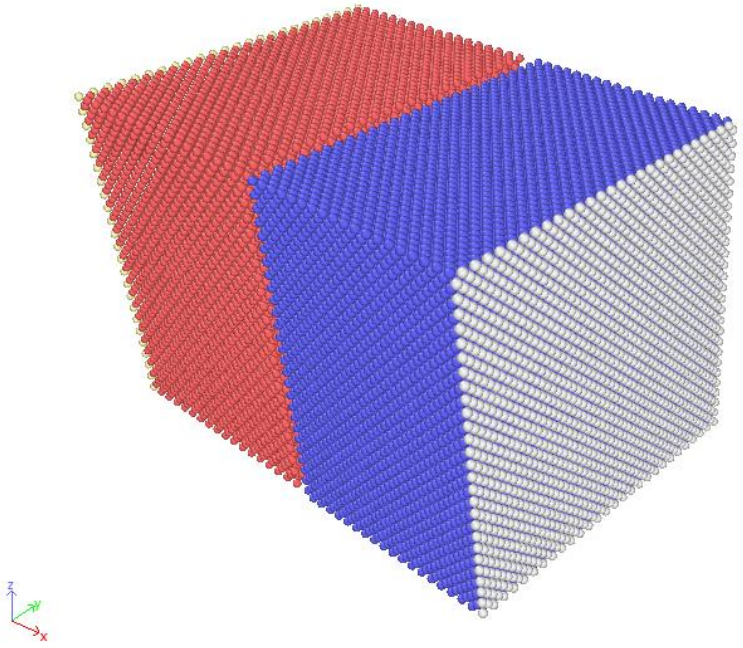

(b)

Fig. 2: Simulation model of Al-Ni and its respective fixed region at (a) top and (b) angle view.

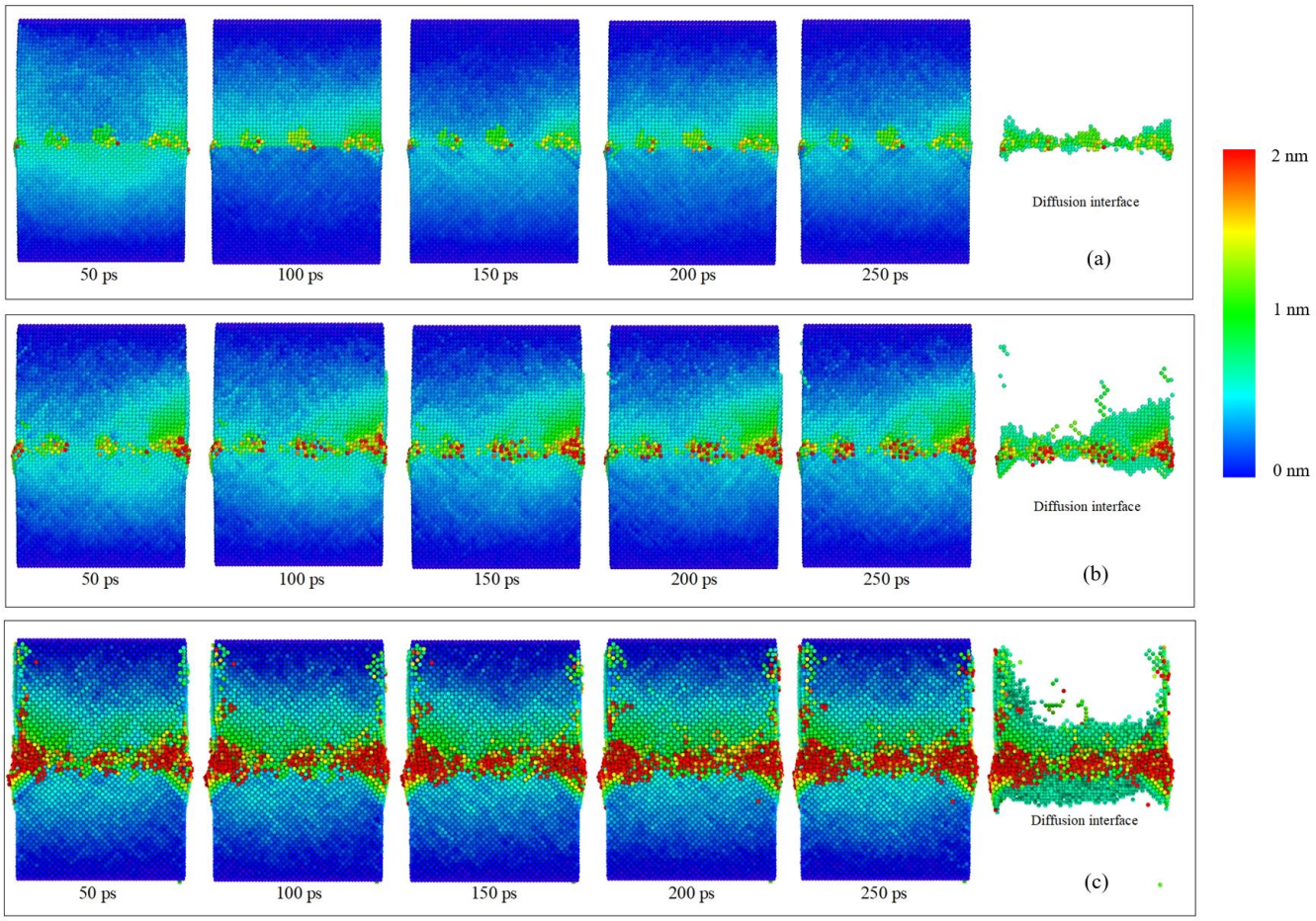

Fig. 3: Sample of structural evolution of Al-Ni slabs during diffusion welding of different temperature of 300 K, 500 K, and 700 K correspond to the (a) S46, (b) S47, and (c) S48, respectively.

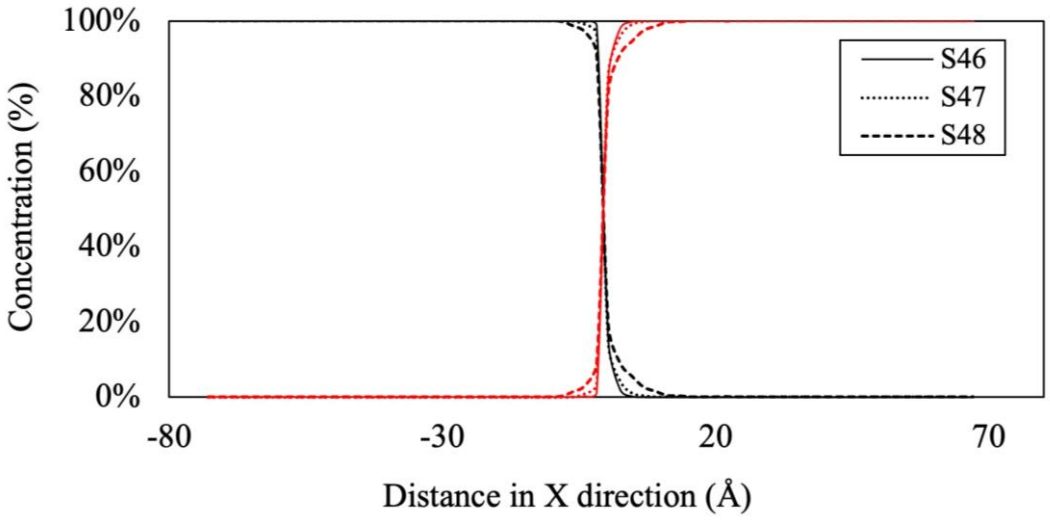

Fig. 4: Samples of concentration distribution of three different welding conditions with different temperature of 300 K, 500 K, and 700 K correspond to the S46, S47, and S48, respectively.

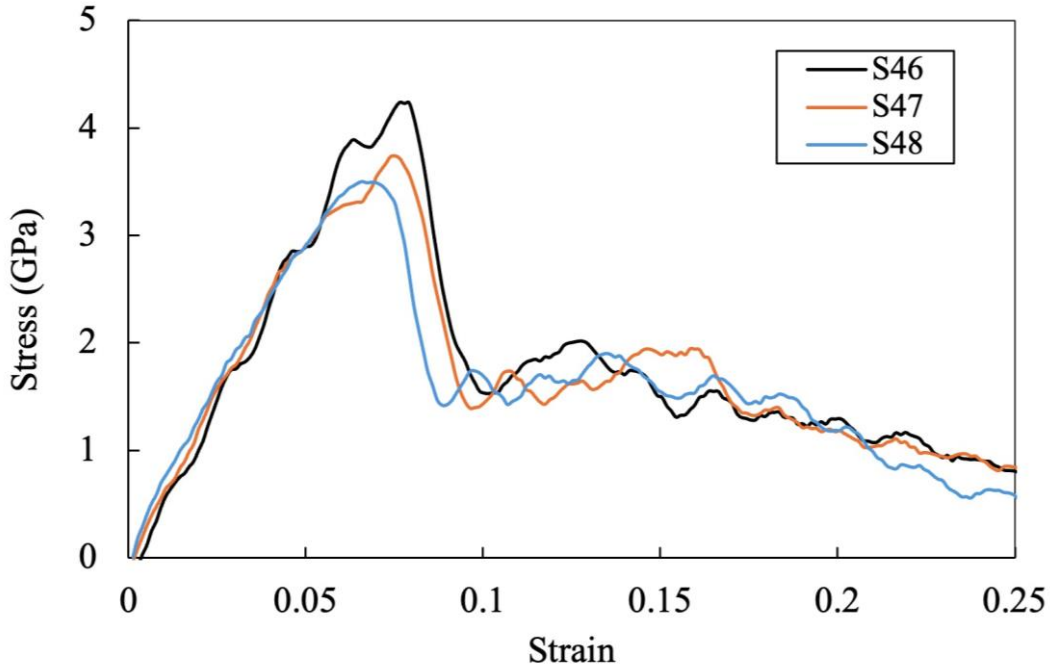

Fig. 5: Samples of stress-strain curve from the tensile test of three different welding conditions with temperature of 300 K, 500 K, and 700 K correspond to the S46, S47, and S48, respectively.

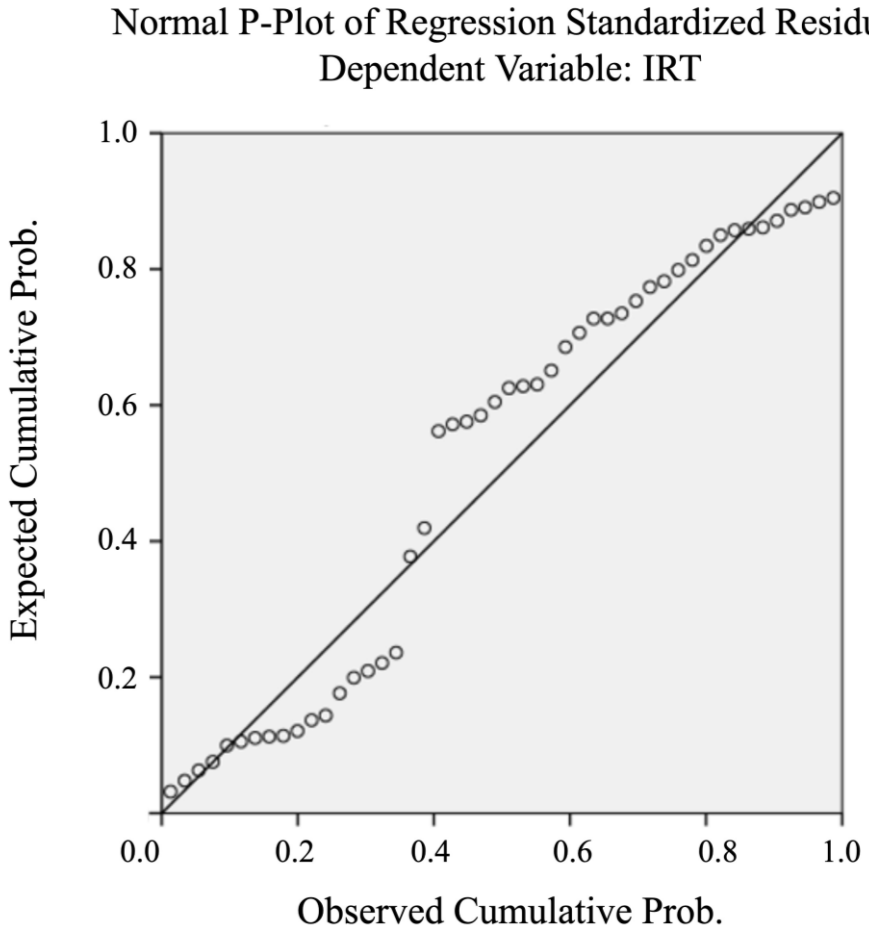
Normal P-Plot of Regression Standardized Residual
Dependent Variable: IRT
Expected Cumulative Prob.
Observed Cumulative Prob.
0.0
0.2
0.4
0.6
0.8
1.0

(a)

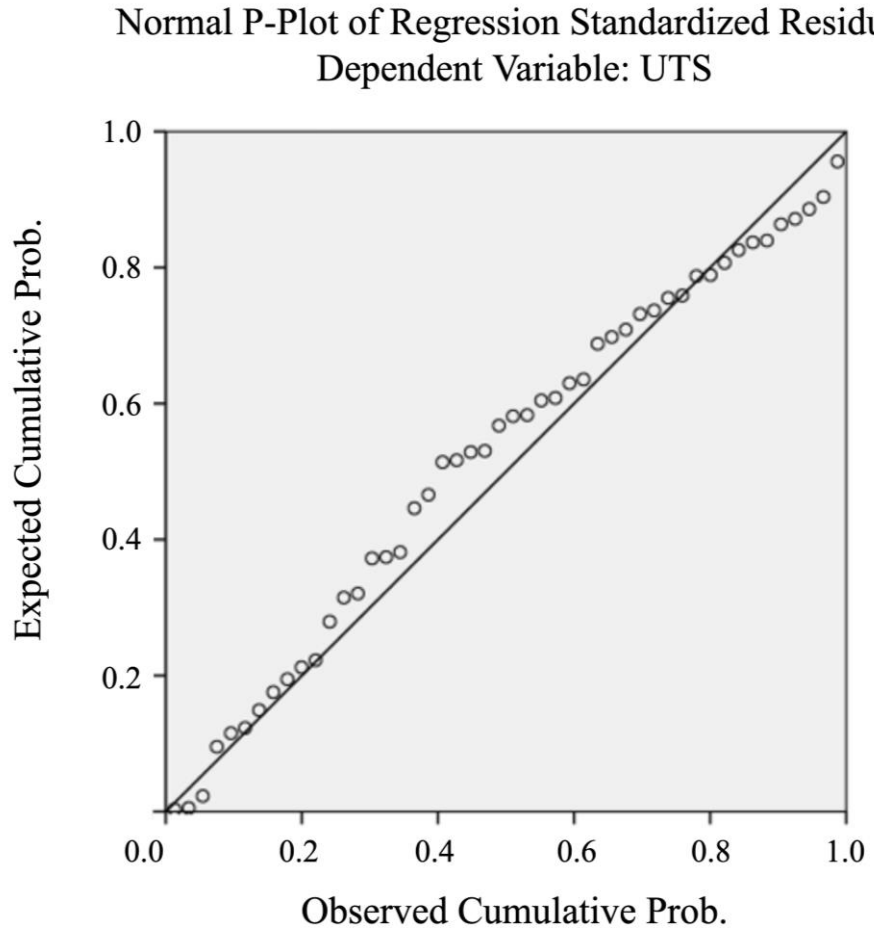

(b)

Fig. 6: P-plot normality test of independent variables (temperature, pressure, and holding time) toward (a) interfacial region thickness and (b) ultimate tensile strength.

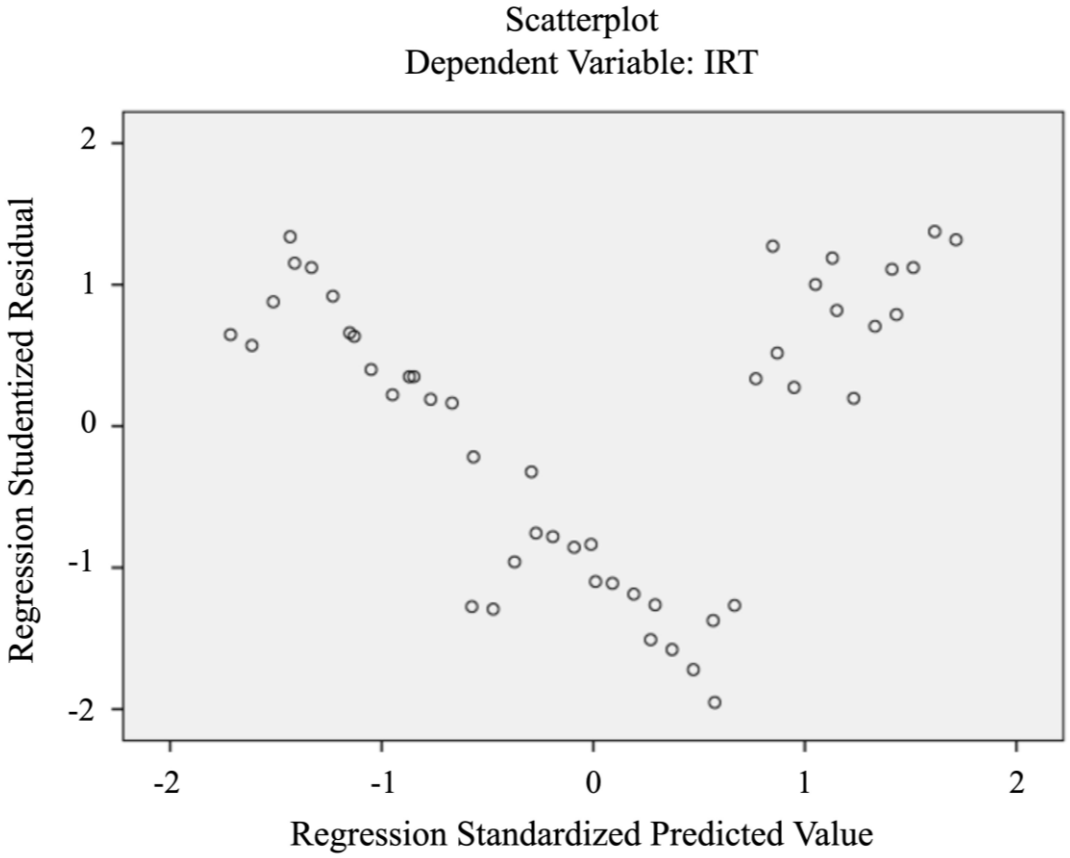
Scatterplot
Dependent Variable: IRT
Regression Studentized Residual
Regression Standardized Predicted Value
2
1
0
-1
-2
-2
-1
0
1
2

(a)

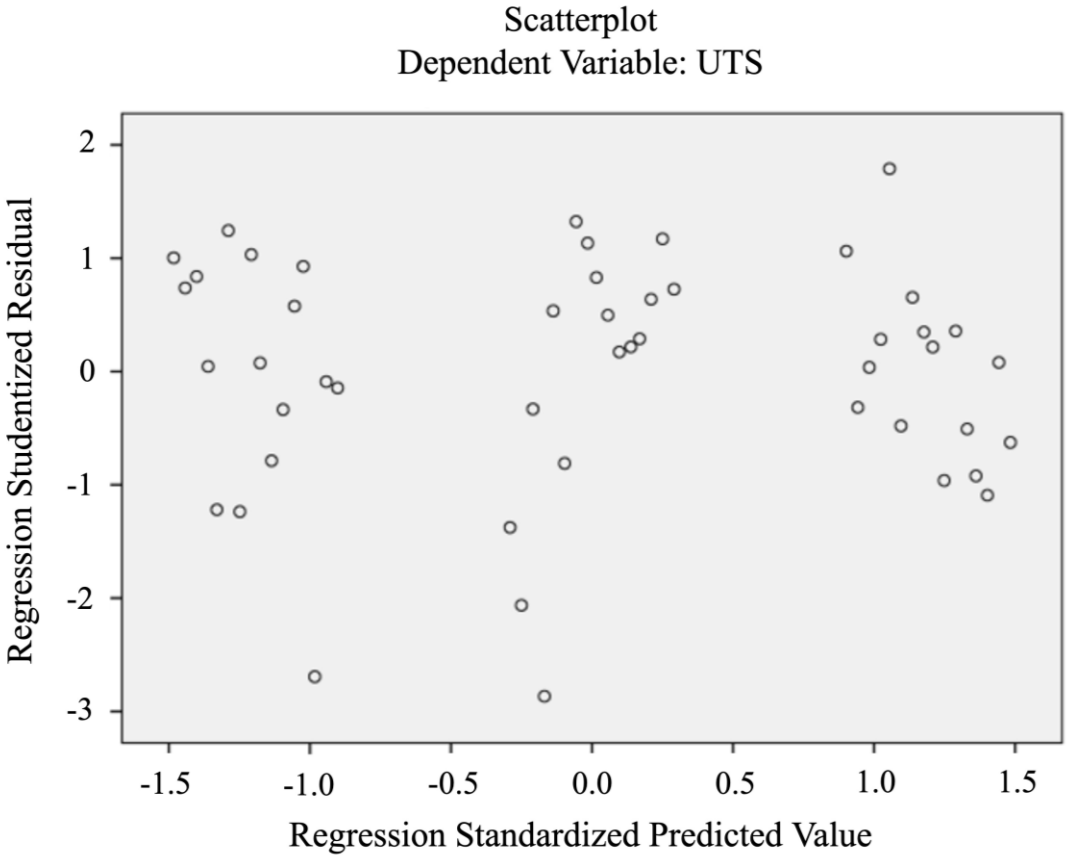

(b)

Fig. 7: Scatterplot of Heteroscedasticity test for (a) interfacial region thickness and (b) ultimate tensile strength.

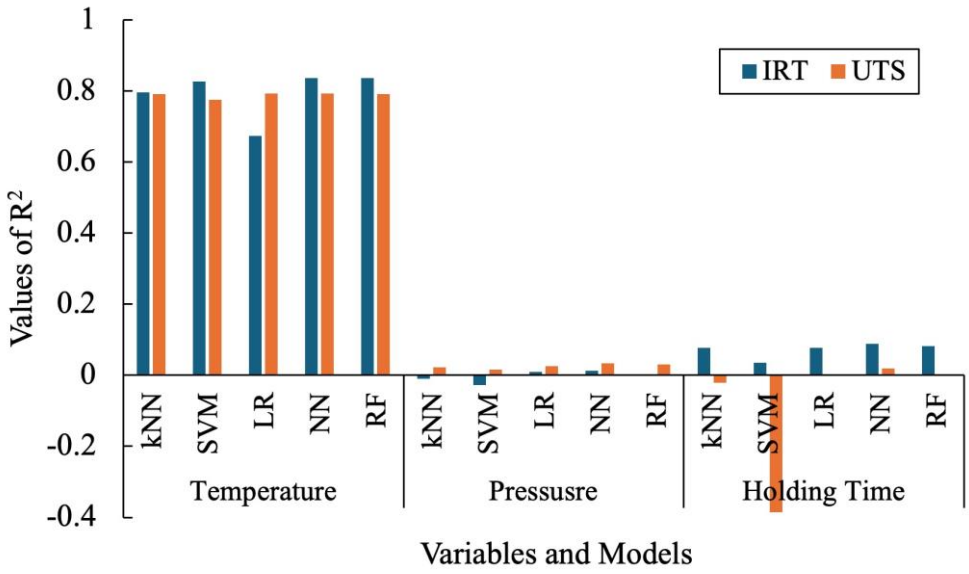

Fig. 8: The value of R^2 of one different independent variables and models of predicting the value of dependent variables.

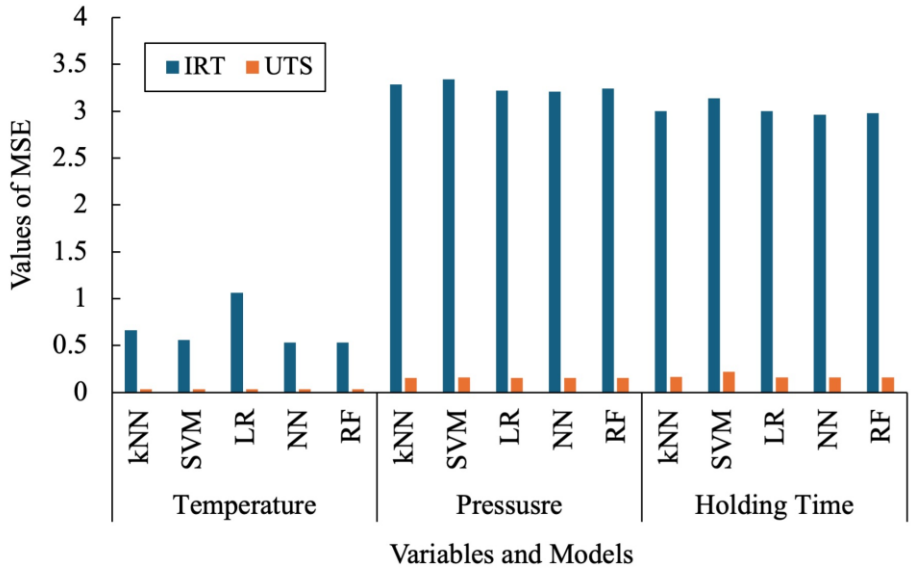

Fig. 9: The value of MSE of one different independent variables and models of predicting the value of dependent variables.

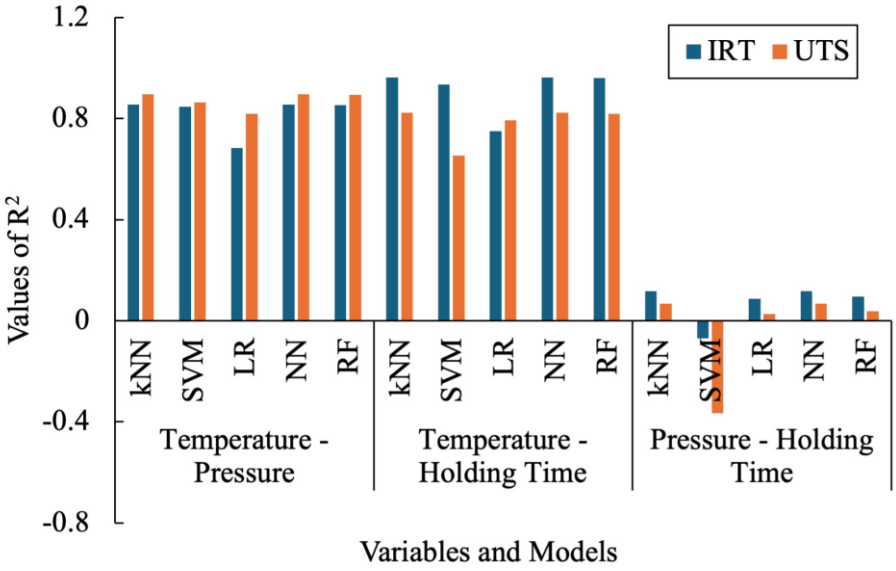

Fig. 10: The value of R^2 of two different independent variables and models of predicting the value of dependent variables.

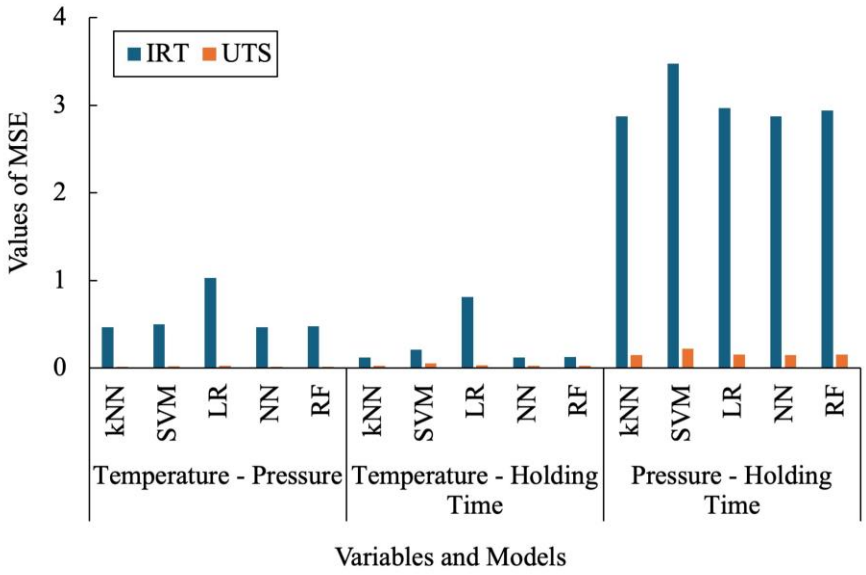

Fig. 11: The value of MSE of two different independent variables and models of predicting the value of dependent variables.

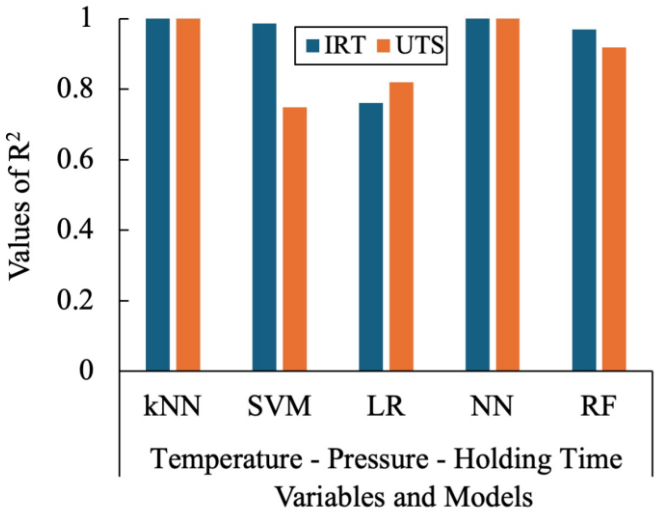

(a)

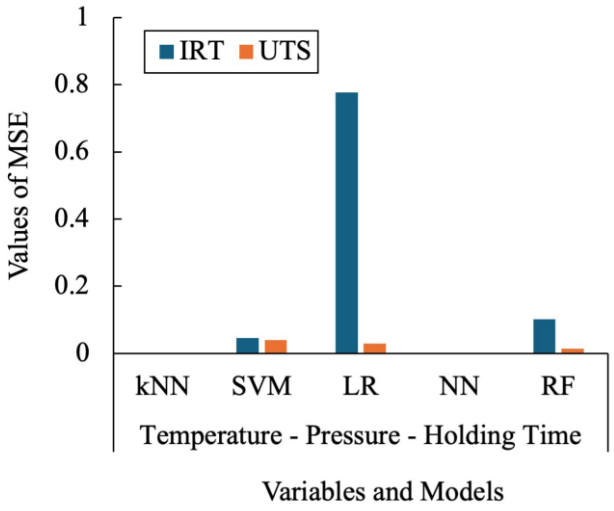

(b)

Fig. 12: The values of (a) R^2 and (b) MSE of three independent variables and models of predicting the value of dependent variables.

Table 1: Simulation parameters and levels.

Level	Simulation Parameters		
	Temperature (K)	Pressure (MPa)	Holding Time (ps)
1	N/A	10	100
2	300	50	150
3	500	100	200
4	700	150	250

Table 2: Detailed simulation parameters in a matrix shape.

Parameters	Holding time 1	Holding time 2	Holding time 3	Holding time 4
Press 1, Temp 1	N/A	N/A	N/A	N/A
Press 1, Temp 2	S1	S13	S25	S37
Press 1, Temp 3	S2	S14	S26	S38
Press 1, Temp 4	S3	S15	S27	S39
Press 2, Temp 1	N/A	N/A	N/A	N/A
Press 2, Temp 2	S4	S16	S28	S40
Press 2,Temp 3	S5	S17	S29	S41
Press 2,Temp 4	S6	S18	S30	S42
Press 3,Temp 1	N/A	N/A	N/A	N/A
Press 3,Temp 2	S7	S19	S31	S43
Press 3,Temp 3	S8	S20	S32	S44
Press 3,Temp 4	S9	S21	S33	S45
Press 4,Temp 1	N/A	N/A	N/A	N/A
Press 4,Temp 2	S10	S22	S34	S46
Press 4,Temp 3	S11	S23	S35	S47
Press 4,Temp 4	S12	S24	S36	S48

Notes:

Temp 1 = N/A
Temp 2 = Temperature at 300 K
Temp 3 = Temperature at 500 K
Temp 4 = Temperature at 700 K

Holding Time 1 = 100 ps
Holding Time 2 = 150 ps
Holding Time 3 = 200 ps
Holding Time 4 = 250 ps

Press 1 = Pressure at 10 MPa
Press 2 = Pressure at 50 MPa
Press 3 = Pressure at 100 MPa
Press 4 = Pressure at 150 MPa

Table 3: List of the simulation results.

Simulation Conditions	Estimated interfacial region thickness (Å)	Ultimate tensile strength (GPa)	Simulation Conditions	Estimated interfacial region thickness (Å)	Ultimate tensile strength (GPa)
S1	3.08	4.218	S25	3.997	4.415
S2	3.218	3.983	S26	4.486	4.166
S3	4.966	3.651	S27	8.087	3.511
S4	3.184	4.352	S28	3.936	4.407
S5	3.342	4.021	S29	4.383	3.938
S6	5.197	3.453	S30	7.381	3.412
S7	3.615	4.563	S31	3.937	4.402
S8	3.801	3.914	S32	4.474	4.084
S9	6.764	3.177	S33	7.996	3.2
S10	3.997	4.38	S34	4.207	4.239
S11	4.155	3.532	S35	4.586	3.738
S12	7.075	3.495	S36	8.218	3.5
S13	4.146	4.201	S37	4.167	4.312
S14	4.496	4.059	S38	4.356	4.102
S15	7.713	3.054	S39	8.447	3.517
S16	4.133	4.164	S40	4.194	4.274
S17	4.235	3.98	S41	4.431	3.96
S18	7.002	3.319	S42	8.636	3.583
S19	4.113	4.191	S43	4.331	4.363
S20	4.327	3.694	S44	4.465	4.062
S21	7.812	3.614	S45	9.02	3.604
S22	4.009	4.164	S46	4.161	4.295
S23	4.285	3.424	S47	4.449	3.324
S24	7.796	3.468	S48	9.108	3.38

Table 4: Settings of the ML techniques employed in this study.

No	ML Techniques	Settings	
1	k-Nearest Neighbor (kNN)	*Parameters*	*Value*
		Number of neighbors	10
		Metric	Chebyshev
		Wight	By distances
2	Support Vector Machine (SVM)	*Parameters*	*Value*
		SVM Type	v-SVM
		Regression cost (*C*)	1
		Complexity bound (*v*)	0.5
		Kernel	Polynomial
		g (gamma, kernel coefficient)	Auto
		c (penalty parameter)	1
		d (degree(s) of polynomial(s))	3.0
		Numerical tolerance	0.001
		Iteration limit	100
3	Linear Regression (LR)	*Parameters*	*Value*
		Fit intercept (unchecking it fixing it to zero)	Yes
		Regularization	Elastic net regression
		Regularization strength	Alpha: 0.0001
		Elastic net mixing	0.5 : 0.5
4	Neural Network (NN)	*Parameters*	*Value*
		Neurons in hidden layers	100
		Activation	ReLu
		Solver	L-BFGS-B
		Regularization, *a*	0.0001
		Maximal number of iterations	200
5	Random Forest (RF)	*Parameters*	*Value*
		Number of trees	10
		Number of attributes considered at each split	Not used
		Replicable training	Not used
		Balance class distribution	Not used
		Growth control	
		Limit depth of individual trees	Not used
		Do not split subsets smaller than	5

Table 5: Tolerance and VIF of multicollinearity test results.

Model		Collinearity Statistics	
		Tolerance	VIF
1	(Constant)		
	Temperature	1,000	1,000
	Pressure	1,000	1,000
	Holding Time	1,000	1,000

Table 6: Comparison of ML techniques of one independent variable to single dependent variable.

Parameters	Interfacial region thickness					Ultimate tensile strength					
	Model	MSE	RMSE	MAE	MAPE	R^2	Model	MSE	RMSE	MAE	MAPE	R^2
Temperature	kNN	0.662	0.814	0.601	0.11	0.796	kNN	0.034	0.183	0.145	0.039	0.792
	SVM	0.56	0.748	0.454	0.091	0.828	SVM	0.036	0.19	0.138	0.037	0.775
	LR	1.062	1.03	0.892	0.183	0.674	LR	0.033	0.183	0.144	0.039	0.793
	NN	0.531	0.729	0.476	0.092	0.837	NN	0.033	0.183	0.143	0.039	0.793
	RF	0.531	0.729	0.475	0.092	0.837	RF	0.033	0.183	0.144	0.039	0.792
Pressure	kNN	3.286	1.813	1.461	0.262	-0.01	kNN	0.157	0.397	0.343	0.092	0.022
	SVM	3.342	1.828	1.695	0.34	-0.027	SVM	0.158	0.398	0.35	0.093	0.016
	LR	3.219	1.794	1.554	0.295	0.01	LR	0.157	0.396	0.345	0.091	0.025
	NN	3.211	1.792	1.557	0.296	0.013	NN	0.156	0.394	0.341	0.09	0.034
	RF	3.242	1.801	1.579	0.303	0.003	RF	0.156	0.395	0.345	0.091	0.031
Holding time	kNN	3.002	1.732	1.49	0.268	0.077	kNN	0.164	0.405	0.353	0.095	-0.021
	SVM	3.14	1.772	1.647	0.326	0.035	SVM	0.223	0.472	0.4	0.104	-0.386
	LR	3.002	1.733	1.552	0.292	0.077	LR	0.161	0.401	0.361	0.096	0.002
	NN	2.963	1.721	1.552	0.291	0.089	NN	0.158	0.397	0.357	0.095	0.019
	RF	2.981	1.727	1.528	0.282	0.083	RF	0.16	0.401	0.354	0.095	0.003

Table 7: Comparison of ML techniques of two independent variables to single dependent variable.

Parameters	Interfacial region thickness					Ultimate tensile strength					
Temperature – Pressure	Model	MSE	RMSE	MAE	MAPE	R^2	Model	MSE	RMSE	MAE	MAPE	R^2
	kNN	0.467	0.684	0.467	0.091	0.856	kNN	0.017	0.129	0.099	0.027	0.897
	SVM	0.498	0.706	0.488	0.097	0.847	SVM	0.022	0.148	0.116	0.031	0.864
	LR	1.028	1.014	0.875	0.178	0.684	LR	0.029	0.171	0.135	0.036	0.818
	NN	0.467	0.684	0.467	0.091	0.856	NN	0.017	0.129	0.099	0.027	0.897
	RF	0.477	0.69	0.458	0.09	0.853	RF	0.017	0.131	0.1	0.027	0.894
Temperature – Holding Time	Model	MSE	RMSE	MAE	MAPE	R^2	Model	MSE	RMSE	MAE	MAPE	R^2
	kNN	0.122	0.349	0.233	0.045	0.963	kNN	0.029	0.169	0.124	0.034	0.822
	SVM	0.213	0.462	0.29	0.057	0.934	SVM	0.056	0.236	0.187	0.05	0.654
	LR	0.811	0.9	0.796	0.165	0.751	LR	0.033	0.182	0.144	0.039	0.794
	NN	0.122	0.349	0.233	0.045	0.963	NN	0.029	0.169	0.124	0.034	0.822
	RF	0.125	0.354	0.243	0.046	0.961	RF	0.029	0.171	0.129	0.035	0.818
Pressure – Holding Time	Model	MSE	RMSE	MAE	MAPE	R^2	Model	MSE	RMSE	MAE	MAPE	R^2
	kNN	2.873	1.695	1.552	0.29	0.117	kNN	0.15	0.388	0.338	0.089	0.067
	SVM	3.475	1.864	1.704	0.341	-0.069	SVM	0.22	0.469	0.403	0.104	-0.366
	LR	2.968	1.723	1.552	0.292	0.087	LR	0.157	0.396	0.345	0.091	0.027
	NN	2.873	1.695	1.552	0.29	0.117	NN	0.15	0.388	0.338	0.089	0.067
	RF	2.941	1.715	1.518	0.278	0.096	RF	0.155	0.394	0.343	0.09	0.037

Table 8: Comparison of ML techniques of three independent variables to single dependent variable.

Parameters	Interfacial region thickness					Ultimate tensile strength					
	Model	MSE	RMSE	MAE	MAPE	R^2	Model	MSE	RMSE	MAE	MAPE	R^2
Temperature – Pressure – Holding Time	kNN	0	0	0	0	1	kNN	0	0	0	0	1
	SVM	0.046	0.215	0.152	0.029	0.986	SVM	0.04	0.201	0.17	0.045	0.749
	LR	0.777	0.882	0.79	0.165	0.761	LR	0.029	0.17	0.134	0.036	0.82
	NN	0	0.001	0.001	0	1	NN	0	0.004	0.002	0.001	1
	RF	0.101	0.318	0.196	0.035	0.969	RF	0.013	0.115	0.09	0.024	0.918

Biographies of all authors:

Mohamad ZAENUDIN: he earned his bachelor's degree from the State University of Jakarta and his master's degree from Management and Science University. Currently, he serves as a senior lecturer in the Department of Mechanical Engineering at Jakarta Global University. His research focuses on the materials science of metallic materials, utilizing the molecular dynamics method.

Dian NUGRAHA: he received his bachelor at State Polytechnic Sriwijaya, and M.IT at Management and Science University. He has win prestigious award from Anugerah Diktisaintek. He is currently working as senior lecturer at the Department of Informatics Engineering, Jakarta Global University. His research focused on multimedia, augmented reality, and computer engineering.

Safira FAIZAH: she received her bachelor at State Polytechnic Sriwijaya, and M.IT at Management and Science University. She is currently working as assistant professor at Jakarta Global University. Her research focused on computer science and engineering, heading the Department of Informatics Engineering.

Adhes GAMAYEL: he received his bachelor's and master's degree from University of Brawijaya and then pursue his doctorate at Management and Science University. He is currently working as associate professor at the Department of Mechanical Engineering, Jakarta Global University. His research focused on renewable energy, such as bio-oil and piezoelectric energy harvester.

Mohammed N. Abdulrazzaq: Dr. Mohammed N. Abdulrazaq Alshekhly is an esteemed Associate Professor at the College of Engineering and the Chair of University Research Council at Gulf University. His journey into academia began with his B.Sc. degree in Mechanical/Production Engineering, which he received from the University of Technology–Baghdad, Iraq, in 2006. He then proceeded to attain a Master's degree in Mechanical Engineering in 2010, followed by a Ph.D. in 2015, both from the National University of Malaysia (UKM). Dr. Mohammed's scholarly contributions to his research fields, which include the Internet of Things (IoT), Robotics, Metal Processing, and Smart cites, have been substantial. To date, he has amassed over 1850 citations and holds an h-index of 22 and an i10-index of 48. His prolific authorship is showcased in his more than 200 publications, encompassing patents, books, chapter reviews, and peer-reviewed papers in journals and conferences.